

Special Smith–Purcell radiation from an open resonator array

This content has been downloaded from IOPscience. Please scroll down to see the full text.

2014 *New J. Phys.* 16 073006

(<http://iopscience.iop.org/1367-2630/16/7/073006>)

[View the table of contents for this issue](#), or go to the [journal homepage](#) for more

Download details:

IP Address: 188.184.3.52

This content was downloaded on 08/07/2014 at 17:39

Please note that [terms and conditions apply](#).

New Journal of Physics

The open access journal at the forefront of physics

Deutsche Physikalische Gesellschaft  | IOP Institute of Physics

Special Smith–Purcell radiation from an open resonator array

Weihao Liu and Zhengyuan Xu

School of Information Science and Technology, University of Science and Technology of China, Anhui, People's Republic of China
E-mail: liuwhao@ustc.edu.cn

Received 1 November 2013, revised 16 March 2014

Accepted for publication 16 June 2014

Published 4 July 2014

New Journal of Physics **16** (2014) 073006

[doi:10.1088/1367-2630/16/7/073006](https://doi.org/10.1088/1367-2630/16/7/073006)

Abstract

An interesting new physical phenomenon is uncovered—an open resonator array excited by an electron beam and able to generate a special kind of Smith–Purcell radiation (SPR). Although the frequency and direction satisfy the SPR relation, this is a single frequency radiation in a specific direction that is essentially different from ordinary SPR. The spectral density of this special radiation is also much higher than that of ordinary SPR. By means of theoretical analysis and digital simulations, the radiation mechanism together with its requirements are explored. This radiation may have great influence in modern physics and optics as it offers new ways to carry out coherent radiation generation and beam diagnostics.

Keywords: Smith–Purcell radiation, open resonators array, coherent radiation

Since its first experimental observation in 1953, Smith–Purcell radiation (SPR), from a uniformly moving electron beam passing over a periodic surface, has been the subject of much theoretical and experimental work for its great applications in radiation generation, beam acceleration and nondestructive diagnostics of electron beams [1–5]. It is characterized by the following well-known dispersion relation:

$$\lambda = -\frac{L}{n} \left(\frac{1}{\beta} - \cos \theta \right) \quad (1)$$



Content from this work may be used under the terms of the [Creative Commons Attribution 3.0 licence](https://creativecommons.org/licenses/by/3.0/). Any further distribution of this work must maintain attribution to the author(s) and the title of the work, journal citation and DOI.

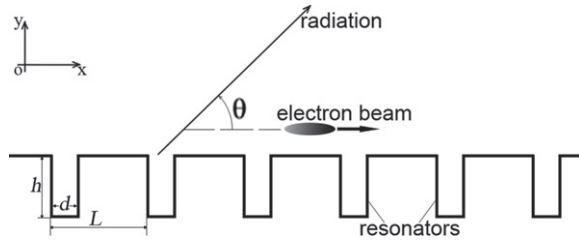


Figure 1. Schematic diagram of the Smith–Purcell radiation from the resonator array. θ indicates the radiation direction.

where λ is the radiation wavelength, θ (shown in figure 1) indicates the radiation direction, L is the structural period, β is the ratio of the beam velocity to light velocity, and n is a negative integer that indicates the harmonic order.

More recently, the Smith–Purcell free electron laser (SP-FEL) [6–8], which is the coherent SPR from premodulated electron bunches (generated previously by the accelerator or by the beam–wave interaction on the periodic surface), has been extensively studied for its potential in generating radiation that can not be easily obtained by other methods, especially for terahertz (THz) wave generation [9, 10]. In SP-FEL, the SPR becomes coherent in some specific directions, where the SPR frequency is harmonic of bunching frequency, and the radiation intensity is remarkably increased since it is proportional to the square of the bunch number. Even to this day, there are still many studies on SPR for its more potential applications [11–14].

Despite the various studies and applications, the physical mechanism of SPR is still under dispute. Traditionally, there are two theoretical models commonly used to deal with the mechanism of SPR. One is the diffraction model [15, 16], where SPR is thought to be the diffraction of the periodic surface to the electron beam's evanescent incident waves. The other is the surface-current model which is based on the image-charge approximation [17, 18]. According to this model, SPR is generated from the surface-current, induced by a moving electron beam, on the periodic structure. Both models can deduce the relation of equation (1).

In this paper we discover a new kind of SPR—the monochrome coherent radiation from an array of periodically arranged open resonators excited by a uniformly moving electron beam, and, by means of theory and simulations, we are going to show that it has a completely new mechanism which is different from both of the theoretical models mentioned above. Without any preprocessing of the electron beam (note that the formation of a prebunched electron beam is the primary challenge for SP-FEL), it can generate coherent radiation with an intensity much higher than ordinary SPR. This new radiation may have many potential applications in generating coherent THz wave radiations.

Figure 1 shows the scheme that we are going to study. At first sight, it is a rectangular optical gating that is commonly used in ordinary SPR. For better illustration and comparison, let us first briefly visit the ordinary SPR process. According to the diffraction model of ordinary SPR, there are both surface waves and radiation waves in diffraction from a grating. The surface waves, whose frequencies are below the threshold of SPR, can only propagate along the grating and cannot radiate into the free space except for the abrupt change of structure [19, 20], while the radiation waves, which are the negative harmonics of diffraction, can radiate into the upper half-space, and the dependence of radiation frequency with direction satisfies equation (1) [21]. By using the particle-in-cell (PIC) code of CST [22], we carried out the simulations of this case

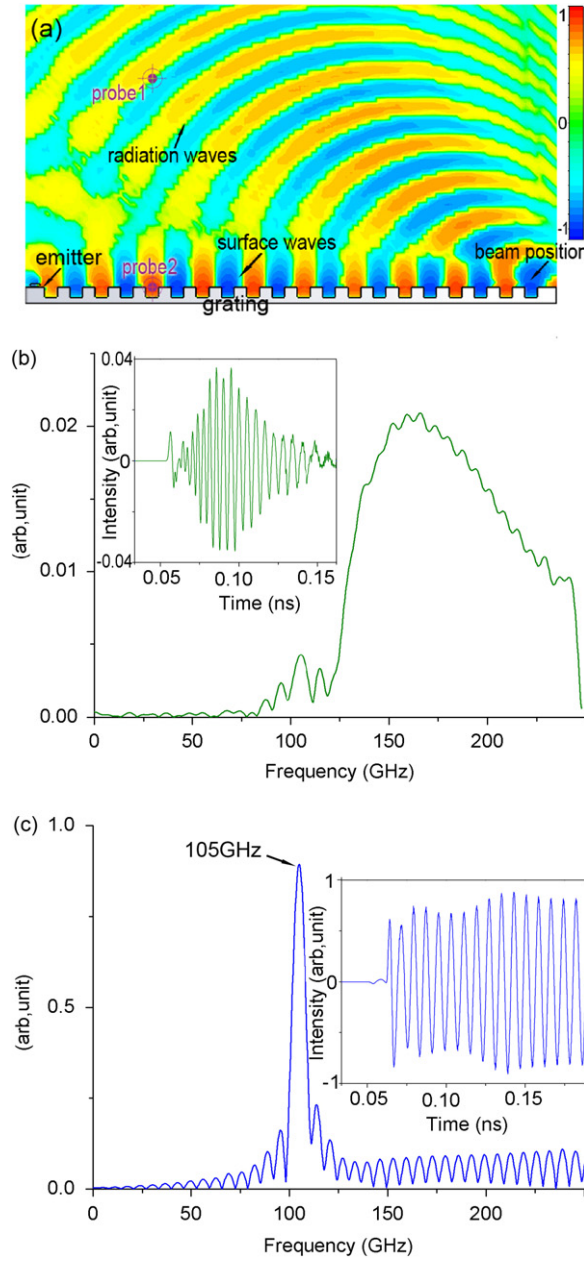


Figure 2. (a) Simulation results for the contour map of the E_x component in ordinary SPR. (b) Simulation results of the radiation spectrum together with the corresponding time-domain waveform, detected by probe 1 shown in figure 2(a). (c) Simulation results of the frequency spectrum of surface waves and the corresponding time-domain waveform, detected by probe 2 shown in figure 2(a).

(hereinafter, case 1) and the results are shown in figure 2, in which the grating is set as a perfect conductor with structural parameters: $L = 1$ mm, $d = 0.5$ mm, $h = 0.4$ mm, and the electron beam is a 2 fs (in time duration) electron pulse with energy 200 keV, which is not hard to obtain experimentally [23].

From the contour map of the electric field (E_x) shown in figure 2(a), we can clearly see that the surface waves and radiation waves are independent of each other: the surface waves are bound to the periodic structure while the radiation waves extend to all directions in the upper half-space. The radiation spectrum, shown in figure 2(b), covers a wide frequency band, which is because the radiation direction is continuously changing while the electron beam is moving. Figure 2(c) shows that the frequency of the surface wave is 105 GHz, which is below the threshold of SPR. These results agree well with theoretical prediction of ordinary SPR.

Now we reduce the gap width d to be 25 μm (all other parameters are kept unchanged) and carry out another simulation (hereinafter, case 2). The results are given in figure 3, which shows that the radiation spectrum changes into a narrow band with peak frequency 172 GHz and the spectrum density increases by a factor of 1.5, see figure 3(b), and the radiation waves in the upper half-space are focused at a specific direction, see figure 3(a). Careful studies show that it is just the corresponding direction ($\theta = 107.8^\circ$) of 172 GHz waves according to equation (1). These results show an interesting phenomenon: the ordinary SPR changes into a monochromatic radiation with enhanced intensity at a specific direction that satisfies the SPR relation. The expansion of the radiation spectrum to the narrow frequency band indicated in simulations can be understood as follows: the electron beam used in simulations is the electron's pulse which results in the excited radiation; it is also a pulse wave (with a finite time duration and a finite time-period number). Under this condition, the radiation spectrum, which is the Fourier transformation of the time-domain pulse waveform, will inevitably extend to a certain frequency bandwidth [24]. To explore the physical mechanism and the characteristics of this new radiation phenomenon are the major goals of this paper.

As is already known, in an open periodic structure of case 1, the surface waves are formed by the coupling of resonator modes in the periodic resonator array [25, 26]. When we reduce the gap width d , the distance between the adjacent resonators will be increased, which will obviously weaken or even eliminate the coupling of the resonator modes. The surface waves will no longer exist when the coupling of the resonator modes are completely eliminated. Under this condition, the grating changes into an array of independent resonators. This can also be illustrated by the dispersion curves shown in figure 4. The dispersion curves of surface waves are a series of curves with positive and negative slopes, respectively, indicating the forward and backward propagating waves on the surface of the periodic structure. While for the resonator modes, the dispersion curves are a series of straight horizontal lines, indicating that they can not propagate along the periodic structure since the group velocity is zero.

Following the above analysis, the mechanism of the new radiation in case 2 can then be uncovered as below. When an electron beam skims over the resonator array, the electromagnetic modes in each resonator of the array will be excited one by one. These resonator modes then independently radiate into the upper half-space, through their open 'mouths' like an antenna array, one after another with a certain phase shift. And the radiation frequencies are just the eigenfrequencies of the resonator modes. The simulation results in figure 3(c) show that the frequency of the resonator modes (172 GHz) is exactly the same as the radiation frequency, which offers a good verification of our analysis. We can also see that, unlike the surface waves whose intensity roughly keeps constant as time elapses (see the inset of figure 2(c)), the intensity of the resonator modes decreases gradually with time (see the inset of figure 3(c)) because of radiation.

Further examination shows that in the direction given by equation (1), the phase shift from every adjacent resonator is $2n\pi$ (n is the integer), indicating that the radiation from all resonators

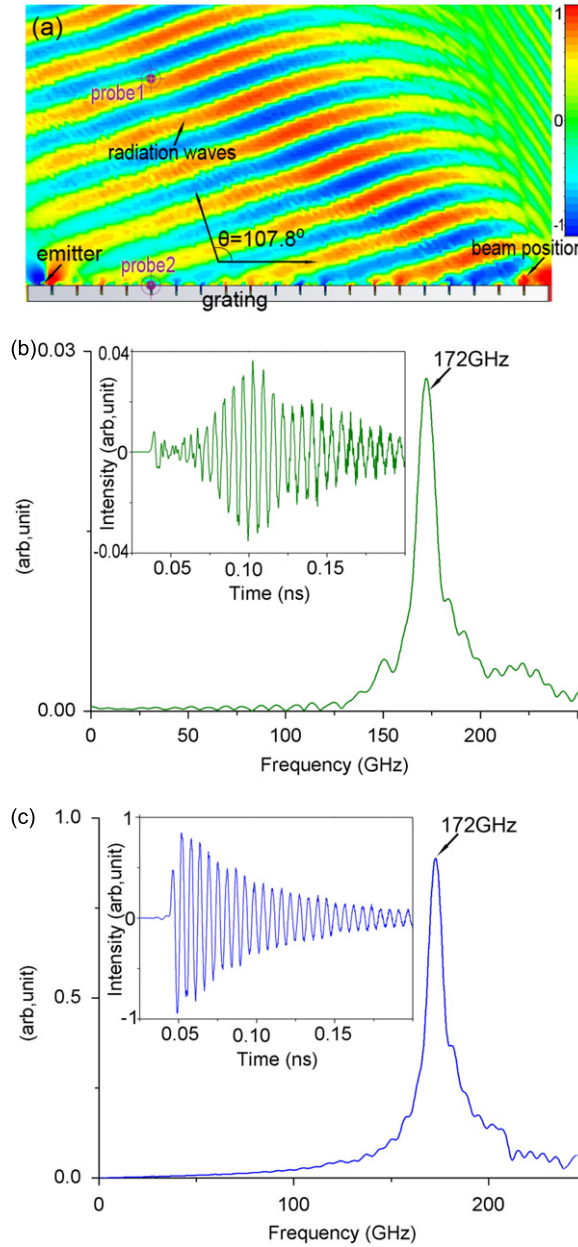


Figure 3. (a) Simulation results for the contour map of the E_x component in special SPR. (b) Simulation results of the radiation spectrum together with the corresponding time-domain waveform, detected by probe 1 shown in figure 3(a). (c) Simulation results of the frequency spectrum of surface waves and the corresponding time-domain waveform, detected by probe 1 shown in figure 3(a).

is coherent. So the radiation in this direction will be remarkably enhanced, while in all other directions the radiations from different resonators will counteract each other, and the radiation can not occur. This is just what we observed in the simulations of case 2, and we will call this new radiation ‘special SPR’ hereinafter.

According to the above analyses, the resonator modes play an essential role in this special SPR since they determine both radiation frequency and direction. Now we study the resonator

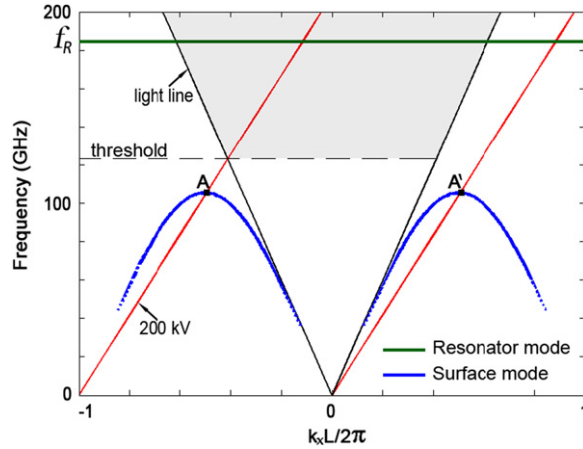


Figure 4. Dispersion curves of the surface waves and of the resonator mode. The f_R is the frequency of the lowest resonator mode, and the shaded part indicates the SPR region.

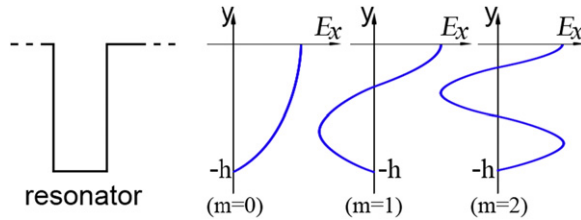


Figure 5. Diagram of a single resonator and the distribution of the E_x component in the y direction for three resonator modes.

modes that can be excited by an electron beam and evaluate their eigenfrequencies. For the case that the gap width is much less than the radiation wavelength, say $d \ll \lambda$, transversal TEM modes (with only two non-zero components, E_x and H_z in the coordinate shown in figure 1) will be primarily excited in the resonators by the electron beam [27, 28]. In other words, the radiations are largely from the transversal TEM modes of resonators. To estimate the eigenfrequencies of these resonator modes, we make the following approximations: the E_x reaches a maximum value at the resonator ‘mouth’, which is reasonable since it is closest to the electron beam, and vanishes at the bottom. According to this approximation, the E_x distributions in the y direction of the resonator can be illustrated by figure 5, from which the wavelength λ of the resonator modes can be determined:

$$\lambda = h \left/ \left(\frac{m}{2} + \frac{1}{4} \right) \right. \quad (2)$$

where m is a non-negative integer, indicating the mode number, and h is the resonator depth.

To verify equation (2) and also to explore the requirements for this special SPR, we have done some simulations for different resonator depths (other parameters are the same as those in case 2). Figure 6 shows the dependence of the resonator mode frequency on resonator depth h and we can see that the frequency increases as h decreases, largely agreeing with the theoretical results obtained by equation (2), in which $m = 0$. Figure 7 further shows the dependence of the

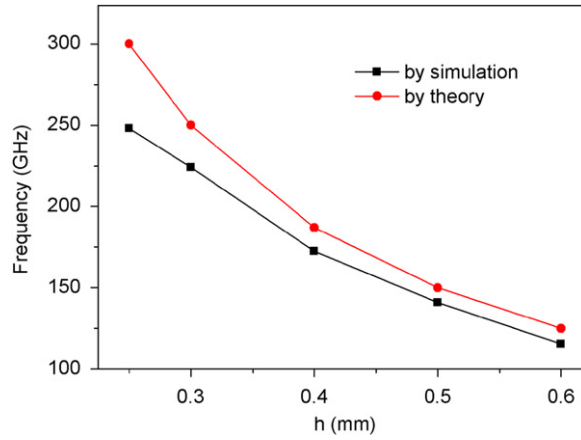


Figure 6. Variations of the resonator mode frequency with resonator depth h . In theory, equation (2) with $m = 0$ is used.

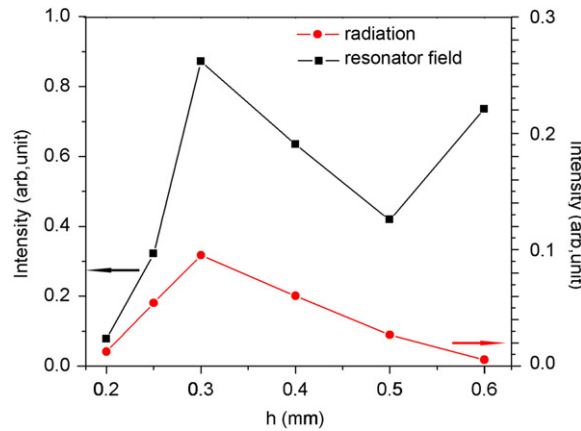


Figure 7. Variations of field intensity at the resonator ‘mouth’ and of the radiation intensity with the resonator depth h . The other parameters are the same as those in figure 3.

field intensity at the resonator ‘mouth’ and of the radiation intensity on the resonator depth h . We can see that, except for the case $h = 0.6$ mm, the radiation is largely in a positive correlation with the resonator field at the ‘mouth’, which is another verification of our claim that the special SPR is from resonator modes. For the case $h = 0.6$ mm, the frequency of the resonator mode is 114 GHz, below the SPR threshold, which means it can not radiate to the upper half-space as with SPR.

Keeping the other parameters the same as those in case 2 ($L = 1$ mm and $h = 0.4$ mm), the intensity variation of special SPR with gap width d are simulated and the results are shown in figure 8, from which we can see that the radiation reaches a relative maximum value at $d = 50 \mu\text{m}$, indicating that d can not be too small or too large. Further simulations show that when $d > 0.1$ mm, the monochromatic special SPR turns into the incoherent ordinary SPR with a wide frequency band because of the coupling of adjacent resonator modes.

Then we keep d and h as constants ($d = 25 \mu\text{m}$ and $h = 0.4$ mm according to case 2), and gradually change the period L . The simulation results of the special SPR intensity variation with

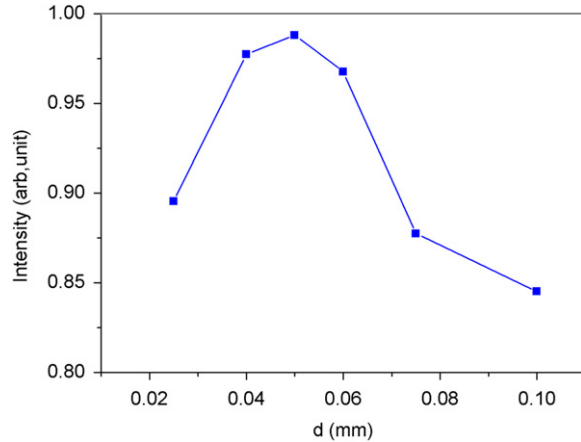


Figure 8. Variations of the radiation intensity with resonator gap width d . Other parameters are the same as those in figure 3.

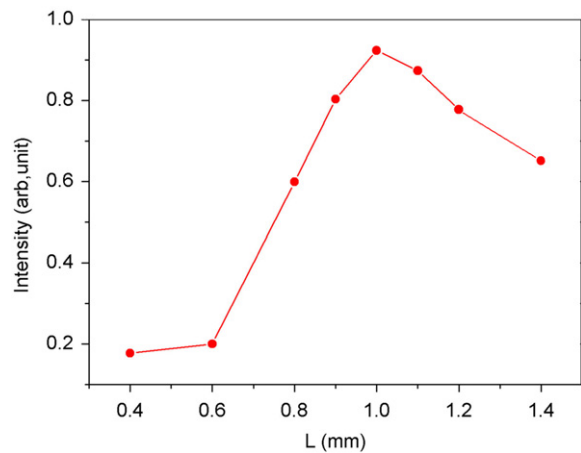


Figure 9. Variations of the radiation intensity with period L . Other parameters are the same as those in figure 3.

L are given in figure 9, which shows that the relative strongest radiation occurs at $L = 1$ mm and, notably, that the radiation intensity drops remarkably when $L < 0.8$ mm. This can be explained as when $L < 0.8$ mm, the SPR threshold increases to be higher than the resonator mode frequency (172 GHz), for example, the SPR threshold is 175 GHz for $L = 0.7$ mm according to equation (1), and under this condition the resonator modes can no longer radiate as SPR. This result is also a good verification of our previous analyses on the mechanism of special SPR.

Based on the simulation results presented above and the new mechanism we have discovered, we can see that for proper operation of the special SPR, the following conditions should be satisfied. 1) The period L and gap width d should be well matched to prevent the coupling of electromagnetic modes in adjacent resonators. 2) The depth of the resonators should be properly chosen: it should be neither too small, where the resonator modes can not be effectively excited, nor be too large, where the resonator mode can not radiate into the upper half-space as SPR since its frequency is below the threshold of SPR. 3) The period L , the

frequency of resonator modes, and the beam velocity should be well matched to satisfy the SPR relation equation (1).

Up to now we have only considered the case of a rectangular grating, i.e., the resonators are all rectangular cavities. In fact, other kinds of resonators can also be used to generate the special SPR based on the mechanism we discussed above. Further investigations will be conducted in the future.

To summarize, an interesting new physical phenomenon has been found—an array of open resonators can generate coherent monochrome radiation via special SPR, which is significantly different from ordinary SPR. The spectral density is much enhanced. By means of theoretical analysis and digital simulations, we demonstrate that it is the coherent radiation from resonator modes. This kind of radiation offers new ways for coherent radiation generation as well as beam diagnostics, so it may have great influence in modern physics and optics.

Acknowledgments

This work was supported in part by National 973 Program of China (grant no. 2013CB329201).

References

- [1] Smith S J and Purcell E M 1953 *Phys. Rev.* **92** 1069–70
- [2] Moran M J 1992 *Phys. Rev. Lett.* **69** 2523
- [3] Castellano M, Verzilov V A, Catani L, Cianchi A, Orlandi G and Geitz M 2001 *Phys. Rev. E* **63** 056501
- [4] Kesar A S 2010 *Phys. Rev. ST Accel. Beams* **13** 022804
- [5] Molenaar P A, van der Straten P, Heideman H G M and Metcalf H 1997 *Phys. Rev. A* **55** 605
- [6] Li D, Hangyo M, Tsunawaki Y, Yang Z, Wei Y, Miyamoto S, Asakawa M R and Imasaki K 2012 *Nucl. Instrum. Meth. Phys. Res. A* **674** 20–23
- [7] Li D, Hangyo M, Tsunawaki Y, Yang Z, Wei Y, Miyamoto S, Asakawa M R and Imasaki K 2012 *Free Electron Lasers (InTech)* Available at: www.intechopen.com/books/free-electronlasers/theoretical-analysis-on-smith-purcell-free-electron-laser
- [8] Korbly S E, Kesar A S, Sirigiri J R and Temkin R J 2005 *Phys. Rev. Lett.* **94** 054803
- [9] Prokop C *et al* 2010 *Appl. Phys. Lett.* **96** 151502
- [10] Andrews H L, Boulware C H, Brau C A and Jarvis J D 2005 *Phys. Rev. ST Accel. Beams* **8** 110702
- [11] Bera A, Barik R K, Min S-H, Kwon O, Baek I, Kim S, Sattorov M A and Park G-S 2012 *Vacuum Electronics (IVEC) 2012 13th IEEE International Conference* pp 157–8
- [12] Liu W and Xu Z 2014 *J. Appl. Phys.* **115** 014503
- [13] Bartolini R *et al* 2012 *J. Instrum.* **7** 01009
- [14] Andrews H L *et al* 2013 *Nucl. Instrum. Meth. Phys. Res. A* **740** 212
- [15] van den Berg P M 1973 *J. Opt. Soc. Am.* **63** 1588
- [16] Haeberle O, Rullhusen P, Salome J M and Maene N 1994 *Phys. Rev. E* **49** 3340
- [17] Brownell J H, Walsh J E and Doucas G 1998 *Phys. Rev. E* **57** 1075
- [18] Karlovets D V and Potylitsyn A P 2006 *Phys. Rev. ST Accel. Beams* **9** 080701
- [19] Gardelle J, Courtois L, Modin P and Donohue J T 2009 *Phys. Rev. ST Accel. Beams* **12** 110701
- [20] Donohue J T and Gardelle J 2005 *Phys. Rev. ST Accel. Beams* **8** 060702
- [21] Liu S, Hu M, Zhang Y, Li Y and Zhong R 2009 *Phys. Rev. E* **80** 036602
- [22] Romanov G 2008 *Proc. LINAC08* (Victoria, BC, Canada)
- [23] Marceau V *et al* 2013 *Phys. Rev. Lett.* **111** 224801
- [24] Jackson J D 1999 *Classical Electrodynamics* 3rd edn (New York: Wiley)

- [25] Tigelis I, Vomvoridis J and Tzima S 1998 *IEEE Trans. Plasma Sci.* **26** 922
- [26] Liu H-C and Yariv A 2012 *Opt. Express* **20** 9249–63
- [27] Liu W, Gong S, Zhang Y, Zhou J, Zhang P and Liu S 2012 *J. Appl. Phys.* **111** 063107
- [28] Zhang K and Li D 2008 *Electromagnetic Theory in Microwave and Optoelectronics* (Berlin: Springer-Velag) pp 426–30